Linearity of index grating recording with spatially oscillating photovoltaic currents

Alexandr Shumelyuk

Institute of Physics, National Academy of Sciences, 03650 Kiev, Ukraine

Ulrich Hartwig and Karsten Buse

Institute of Physics, University Bonn, D-53115 Bonn, Germany

Serguey Odoulov

Institute of Physics, National Academy of Sciences, 03650 Kiev, Ukraine

Theo Woike

Institute of Physics, University Bonn, D-53115 Bonn, Germany

The response of photorefractive crystals with bulk photovoltaic charge transport is usually highly nonlinear, and for illumination with a sinusoidal light pattern the recorded space-charge gratings possess, apart from the principal spatial frequency **K**, several higher spatial harmonics, **2K**, **3K**, etc. We show experimentally that purely sinusoidal index gratings can be recorded in $LiNbO_3$:Fe when the charge redistribution is governed by spatially oscillating photovoltaic currents. This property is especially beneficial for holographic data storage. © 2006 Optical Society of America

OCIS codes: 190.5330, 190.7070.

1. INTRODUCTION

The remarkable photorefractive nonlinearity of iron-doped lithium niobate is caused by a strong bulk photovoltaic effect.[1,2] The effective driving field E_{pv} that redistributes photoexcited charge carriers can exceed 100 kV/cm, as confirmed in recent experiments.[3] Large light-induced electro-optic variations of the refractive index are an obvious advantage of this material, as they ensure high diffraction efficiency and large dynamic range (see, e.g., Ref. 4). At the same time the holograms recorded in $LiNbO_3$:Fe suffer from optical damage (a strong nonlinear lens deteriorates the transmitted beam),[5] intermodulation noise (ghost images appear in the reconstructed waves),[6] and the nonlinearity of the response (the recorded grating is not sinusoidal).[6]

The first two of the above-mentioned undesirable effects can be overcome by using periodically poled $LiNbO_3$:Fe that has a drastically reduced response at low spatial frequencies.[7,8] We report in this paper that the problem of the nonlinearity can be solved by using a grating recording with two orthogonally polarized eigenwaves of the crystal. One ordinary and one extraordinary wave are employed. The improved linearity for such a grating recording was predicted theoretically long ago[9] but was never proved experimentally.

2. QUALITATIVE DESCRIPTION

The nonlinearity of $LiNbO_3$:Fe is due to the formation of space-charge fields E_{sc} that modulate the high-frequency permittivity ϵ via the Pockels effect.[2,10] The Cartesian component of the permittivity tensor can be expressed as follows:

$$\delta\epsilon_{mn}(\mathbf{r}) \simeq -n^4 r_{mnl} E_l(\mathbf{r}), \tag{1}$$

where r_{mnl} is a component of the electro-optic tensor and the difference in ordinary and extraordinary refractive indices is neglected, $n_o \simeq n_e \simeq n$. The space-charge field, in turn, appears as a consequence of charge redistribution by the bulk photovoltaic current j_{ph} (Ref. 2):

$$E_{sc} = -\frac{j_{ph}}{\sigma_{ph}}, \tag{2}$$

with the photoconductivity $\sigma_{ph} = \kappa I$ in the denominator (κ is the specific photoconductivity, its possible anisotropy is neglected, and I is the light intensity). The mth component of the photovoltaic current j_m is[2]

$$j_m = \beta_{mnl} A_n A_l^*, \tag{3}$$

where A is a slowly varying complex amplitude of the electric field vector of the light such that $I \propto |A|^2$, and β_{mnl} is a component of the photovoltaic tensor[2] that may be real or imaginary:

$$\beta_{mnl} = \beta_{mnl}^L + i\delta_{mnk}\beta_{kl}^C, \tag{4}$$

with the unit antisymmetric tensor δ_{mnk} and the real tensors β^L and β^C that describe the so-called linear (L) and circular (C) photovoltaic currents.[2]

The photovoltaic tensor in $LiNbO_3$:Fe possesses both diagonal components (with the identical two last indices, e.g., β_{333}^L, β_{311}^L, β_{222}^L) and nondiagonal components (like β_{131}^L or β_{12}^C). The latter allow for grating recording with orthogonally polarized light waves, one ordinary and the other extraordinary.[11]

The photovoltaic current excited by two orthogonally polarized light waves is spatially oscillating; the direction of its propagation alternates in every half-period of polarization fringes. At the same time, the overall light intensity is distributed uniformly throughout the sample, because interference of orthogonally polarized waves does not lead to an intensity modulation. Thus, as one can see from Eq. (2), the space-charge field distribution in the sample is directly proportional to the variation of photovoltaic current, as the photoconductivity in the denominator does not depend on the spatial coordinate. In other words, the space-charge field and therefore the high-frequency permittivity linearly reproduce the sinusoidally modulated photovoltaic current.

Note that such a linearity is quite unusual for photorefractive crystals: For the majority of intensity-dependent charge-transport processes the photoconductivity is not uniform throughout the sample, and the space-charge field distribution given by Eq. (2) can be considered to be nearly sinusoidal only in the case of small contrast of the recording fringes.

3. EXPERIMENTAL VERIFICATION AND DISCUSSION

To prove the validity of the presented arguments, we analyze diffraction from space-charge gratings recorded with two orthogonally polarized waves and compare it with the diffraction from gratings recorded with identically polarized waves. Particular attention is paid to possible diffraction from gratings with doubled and tripled spatial frequencies that should arise when the photorefractive response is nonlinear and that must be completely suppressed for linear recording.

In the experiment we profit from the possibility to observe anisotropic light diffraction (diffraction with a polarization turned with respect to the polarization of the incident readout beam) from an isotropically recorded grating and, conversely, to observe the isotropic diffraction from the anisotropically recorded grating. This allows us, as it will be clear from what follows, to enhance or to inhibit the diffraction efficiency from any given space-charge grating by appropriate choice of the electrooptic coefficient.

The index gratings are recorded in periodically poled $LiNbO_3$ (PPLN) crystals doped with Y and Fe (0.74 wt. % and 0.06 wt. % in the melt, respectively) with unexpanded beams of a frequency-doubled diode-pumped cw Nd^{3+}YAG laser (TEM_{00}, single frequency, about 100 mW output power, ~ 1.4 mm beam diameter). The PPLN sample is 0.5 mm thick with a domain lattice period of about 16 μm. The domain walls are parallel to the axis of spontaneous polarization and normal to the x axis.

Two recording beams with the intensity ratio 1:1 impinge upon the input face of the X cut sample to record gratings with grating vectors perpendicular to the spontaneous polarization axis. The beams are polarized either identically (ordinary waves inside the sample) or orthogonally (one ordinary and other extraordinary wave). In the first case the recording waves enter the sample symmetrically (at the angles $\pm\theta$) and form a grating with the grating vector $\mathbf{K}=\mathbf{k_1^o}-\mathbf{k_2^o}$ inside the sample [see the wavevector diagram, Fig. 1(a)]. In the second case they are tilted deliberately in order to align the grating vector $\mathbf{K}=\mathbf{k_1^e}-\mathbf{k_2^o}$ parallel to the sample input face [see the wavevector diagram of Fig. 1(c)]. The angles of the recording beams inside the sample are $\theta-\beta$ and $\theta+\beta$, with β being the angle between the bisector of the recording beams and sample face normal. Here $\mathbf{k_1^e}$ and $\mathbf{k_2^o}$ are the wave vectors of the recording waves 1 and 2, and superscripts o and e denote ordinary and extraordinary wave polarizations.

Whenever a permittivity grating with grating vector $\mathbf{K}$ is recorded (isotropically or anisotropically) it can be reconstructed (anisotropically or isotropically) at specially selected readout angles α. The first subscript, i or a, denotes the type of diffraction (isotropic or anisotropic, respectively), and the second subscript, 1 or 2, denotes two possible readout angles. Furthermore, depending on the type of recording (linear or nonlinear) higher harmonics of this grating with grating vectors $\mathbf{2K}$ and $\mathbf{3K}$ might be revealed at appropriate angles. The number of the spatial harmonic $N=1,2,3$, etc. is shown as a superscript of the readout angle. Relevant wave-vector diagrams are shown in Fig. 1. Note that these diagrams are designed for wave vectors inside the crystal. Thus to calculate the diffraction angles, the refraction at the input face should be taken into account. In what follows we keep the same notations for the angles in air as that used before, for the angles inside the crystal, to avoid too many subscripts or superscripts.

To calculate the diffraction angles for readout of the gratings $\mathbf{K}$, $\mathbf{2K}$, and $\mathbf{3K}$, it is convenient to define first the spatial frequency K of the gratings (modulus of the grating vector $\mathbf{K}$) and the tilt angles ψ of the gratings vectors $\mathbf{K}$ with respect to the sample input face:

$$\frac{\lambda^2 K_{i,a}^2}{4\pi^2} = \{[n_o^2 - \sin^2(\beta - \theta)]^{1/2} - [n_{o,e}^2 - \sin^2(\beta + \theta)]^{1/2}\}^2$$

$$+ [\sin(\beta - \theta) - \sin(\beta + \theta)]^2, \tag{5}$$

$$\tan\psi_{i,a} = \frac{[n_o^2 - \sin^2(\beta + \theta)]^{1/2} - [n_{o,e}^2 - \sin^2(\beta - \theta)]^{1/2}}{\sin(\beta + \theta) - \sin(\beta - \theta)}. \tag{6}$$

With K and ψ known one can calculate the dependences of the diffraction angles on recording angles for the isotropic readout

$$\sin\alpha_{i1,2}^N = n_o \sin\left[\psi \pm \arcsin\left(\frac{NK\lambda}{4\pi n_o}\right)\right], \tag{7}$$
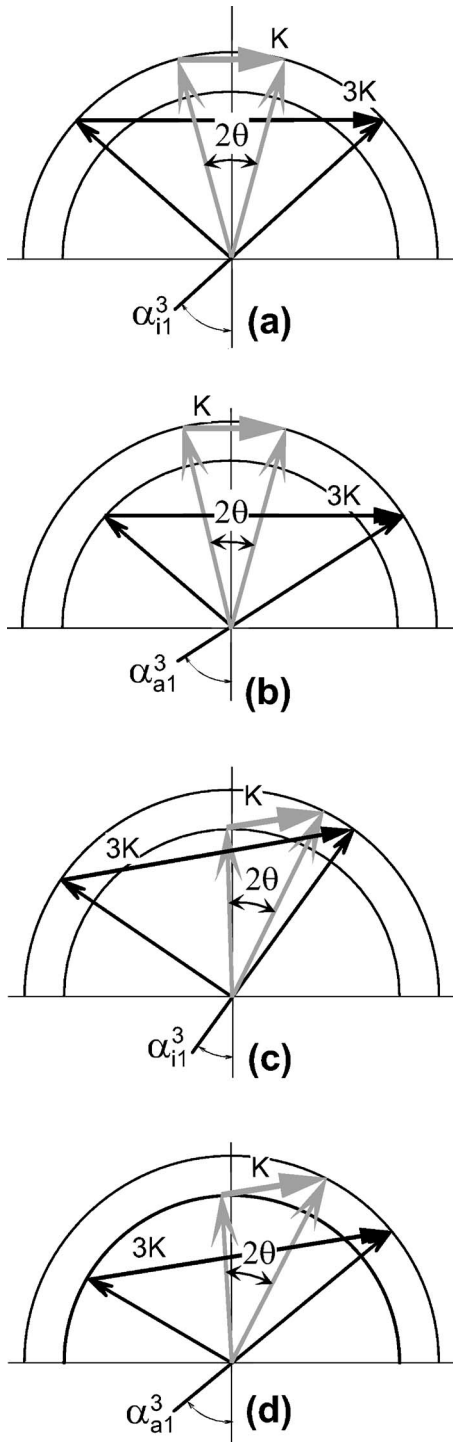
and for the anisotropic readout

Figure 2 shows these calculated dependences together with the experimental data (where diffraction was detected). The simplest case of isotropic recording and isotropic readout is shown in Fig. 2(a). Here, apart from Bragg diffraction from the principal gratings **K**, strong diffraction is also observed from the gratings with doubled and tripled spatial frequencies [see the wavevector diagram of Fig. 1(a)]. The measured Bragg angles for these gratings $\alpha_{i1,2}^1$, $\alpha_{i1,2}^2$, and $\alpha_{i1,2}^3$ are in good agreement with the ones calculated from Eq. (7) for $N=1,2,3$ and symmetric incidence, i.e., with $\psi=0$.

The isotropically recorded grating and their higher harmonics allow also anisotropic readout [see Fig. 1(b)] at the angles $\alpha_{a1,2}^1$, $\alpha_{a1,2}^2$, and $\alpha_{a1,2}^3$; Fig. 2(b). Once more, good agreement of the measured angles with the ones calculated from Eq. (8) for $N=1,2,3$ can be stated.

Fig. 1. Phase-matching diagrams for diffraction from (a), (b) isotropically and (c), (d) anisotropically recorded gratings. Gray arrows show the recording processes. For every diagram in (b), (c), and (d) only one of two possible readout angles is shown for the third spatial harmonic (grating vector **3K**), α_{i1}^3 and α_{a1}^3, respectively, for isotropic and anisotropic readout.

$$\sin\alpha_{a1,2}^N = n_{o,e}\sin\left\{\begin{array}{l}\mp\psi\\[2mm]+\arcsin\left[\dfrac{(4\pi^2 n_{e,o}^2/\lambda^2 - 4\pi^2 n_{o,e}^2/\lambda^2 + N^2 K^2)^{1/2}}{2NKn_{e,o}}\right]\end{array}\right\}.$$
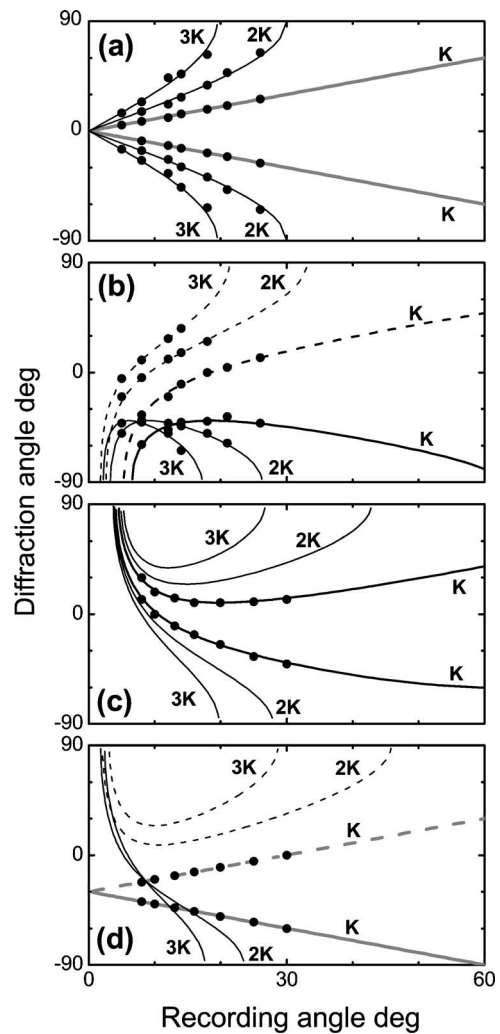
(8)

Fig. 2. Diffraction angles (in air) versus angle between the recording beams (in air) for (a), (b) isotropic recording and (c), (d) anisotropic recording for (a), (c) isotropic readout and (b), (d) anisotropic readout. The calculated dependencies are shown by curves (solid curves for readout with ordinarily polarized waves, dashed curves for readout with extraordinarily polarized waves), whereas dots show the angles measured in the experiment. The dependences shown in gray mark the cases in which the readout angles coincide with the recording angles. **K**, **2K**, and **3K** denote dependences for fundamental (**K**) and high-order (**2K**, **3K**) spatial harmonics.

Table 1. Diffraction Efficiency η for the K, 2K, and 3K Gratings for Different Recording and Readout Conditions[a]

Recording → Readout ↓	$i(o,o)$	$a(o,e)$
$i1(o,o)$	0.0025	0.002
$i2(o,o)$	0.001	<0.00001
$i3(o,o)$	0.00006	<0.00001
$a1(o,e)$	0.004	0.08
$a2(o,e)$	0.0024	<0.00001
$a3(o,e)$	0.0003	<0.00001

[a]*i*, isotropic; *a*, anisotropic; o, ordinary polarization; e, extraordinary polarization

Figure 2(c) shows dependences calculated for anisotropic readout of the anisotropically recorded principal gratings **K**, and the anisotropic readout of their possible higher harmonics [Eq. (8) with $N=1,2,3$]. In spite of the fact that for recording angles within the range of 5° to 20° the calculated diffraction angles are quite reasonable (not exceeding ±60°) we have not detected any diffraction neither from **3K** nor from **2K** gratings. When reading out isotropically the anisotropically recorded gratings [see phase diagram of Fig. 1(c) and Eq. (7)] similar results were obtained; only the principal gratings **K** showed up with no diffraction from the **2K** and **3K** gratings [Fig. 2(c)].

With the optical quality of the photorefractive sample used, the smallest diffraction efficiency η that can be measured is about 10^{-5}. From visual observation of a diffracted spot on the background of scattered light even smaller values of η can be detected. Within this accuracy, in full agreement with our expectations, no diffraction has been observed from the **2K** and **3K** gratings in case of anisotropic recording.

To give the reader an idea about how strong the considered permittivity gratings are, Table 1 summarizes the saturated diffraction efficiencies for different recording and readout conditions.

As one can see, the efficiency of anisotropic readout is always larger than that for isotropic readout. This is quite understandable, as the relevant electrooptic coefficient for anisotropic readout, $r_{42} \approx 33 \pm 3$ pm/V, is larger than that for isotropic readout, $r_{22} \approx 6.7 \pm 0.2$ pm/V.[12] The vanishing of the diffraction efficiency for anisotropic recording of the **2K** and **3K** gratings is significant.

4. CONCLUSION

To summarize, we proved experimentally the linearity of the photorefractive response of $LiNbO_3$:Fe crystals, which is due to circular bulk photovoltaic currents that are a consequence of the nonvanishing antisymmetric components of the photovoltaic tensor.[2] Any other photorefractive gratings that are recorded with two orthogonally polarized eigenwaves of the crystal should possess this property, too. In $LiNbO_3$ this applies to the recording of gratings with the grating vectors **K** aligned along the crystallographic x axis and perpendicular to the axis of spontaneous polarization. Here one of the recording beams is polarized along the x axis and the other along the y axis.[13] Grating recording in this particular geometry is of importance, because it can be useful for distributed-feedback optical parametric oscillators in periodically poled $LiNbO_3$ crystals.[14]

REFERENCES

1. A. M. Glass, D. von der Linde, and T. J. Negran, "High-voltage bulk photovoltaic effect and the photorefractive process in LiNbO₃," Appl. Phys. Lett. **25**, 233–234 (1974).
2. B. I. Sturman and V. M. Fridkin, *The Photovoltaic and Photorefractive Effects in Noncentrosymmetric Materials* (Gordon and Breach, 1992).
3. Marc Luenemann, Ulrich Hartwig, and Karsten Buse, "Improvements of sensitivity and refractive-index changes in photorefractive iron doped lithium niobate crystals by applications of extremely large external electric fields," J. Opt. Soc. Am. B **20**, 1643–1648 (2003).
4. G. T. Sincerbox, "History and Physical Principles," in *Holographic Data Storage*, J. H. Coufal, D. Psaltic, and G. T. Sincerbox, eds. (Springer, 2000), pp. 3–59.
5. A. Ashkin, G. D. Boyd, J. M. Dzedzich, R. G. Smith, A. A. Ballman, J. J. Levinstein, and K. Nassau, "Optically-induced refractive index inhomogeneities in LiNbO₃ and LiTaO₃," Appl. Phys. Lett. **9**, 72–74 (1966).
6. R. J. Collier, C. B. Burckhardt, and L. H. Lin, *Optical Holography* (Academic, 1971).
7. S. Odoulov, T. Tarabrova, A. Shumelyuk, I. I. Naumova, and T. O. Chaplina, "Photorefractive response of bulk periodically poled LiNbO₃:Y:Fe at high and low spatial frequencies," Phys. Rev. Lett. **84**, 3294–3297 (2000).
8. M. Werner, Th. Woike, M. Imlau, and S. Odoulov, "Holographic recording with reduced intermodulation noise in periodically-poled lithium niobate," Opt. Lett. **30**, 610–612 (2005).
9. A. Novikov, S. G. Odoulov, O. Oleinik, and B. I. Sturman, "Beam coupling, four-wave mixing and optical oscillation due to spatially oscillating photovoltaic currents in lithium niobate crystals," Ferroelectrics **75**, 295–315 (1987).
10. L. Solymar, D. J. Webb, and A. Grunnet-Jepsen, *The Physics and Applications of Photorefractive Materials* (Clarendon, 1996).
11. S. Odoulov, "Spatially oscillating photovoltaic current in iron-doped lithium niobate crystals," JETP Lett. **35**, 10–13 (1982).
12. M. Jazbinšek and M. Zgonik, "Material tensor parameters of LiNbO₃ relevant for electro- and elasto-optics," Appl. Phys. B **74**, 407414 (2002).
13. S. G. Odulov and O. I. Oleĭnik, "Dynamic holograms formed in LiNbO₃ crystals by the transverse photogalvanic effect," Sov. J. Quantum Electron. **13**, 980–982 (1983).
14. A. C. Chiang, Y. Y. Lin, T. D. Wang, Y. C. Huang, and J. T. Shy, "Distributed-feedback optical parametric oscillation by use of a photorefractive grating in periodically poled lithium niobate," Opt. Lett. **27**, 1815–1817 (2002).